Elastic Properties, Mechanical Stability, and State Densities of Aluminnides

B.R. Zhang[a], Z. Jia[a], X.Z. Duan[b,*] and X.Z. Yang[a]

[a]Aviation General Hospital, Beijing, 100012, China

[b]Beijing Tongren Hospital, Beijing, 100730, China

First-principles calculations were performed to study on alloying stability, electronic structure, and mechanical properties of Al-based intermetallic compounds. The results show that the lattice parameters obtained after full relaxation of crystalline cells are consistent with experimental data. The calculation of cohesive energies indicated that the structure stability of these Al-based intermetallics will become higher with increasing Zr element in crystal. The calculations of formation energies showed that $AlCu_2Zr$ has the strongest alloying ability, followed by $AlZr_3$ and finally the $AlCu_3$. Further analysis finds out that single-crystal elastic constants at zero-pressure satisfy the requirement of mechanical stability for cubic crystals. The calculations on the ratio of bulk modulus to shear modulus reveal that $AlCu_2Zr$ can exhibit a good ductility, followed by $AlCu_3$, whereas $AlZr_3$ can have a poor ductility; however, for stiffness, these intermetallics show a converse order. The calculations on Poisson's ratio show that $AlCu_3$ is much more anisotropic than the other two intermetallics. In addition, calculations on densities of states indicates that the valence bonds of these intermetallics are attributed to the valence electrons of Cu $3d$ states for $AlCu_3$, Cu $3d$ and Zr $4d$ states for $AlCu_2Zr$, and Al $3s$, Zr $5s$ and $4d$ states for $AlZr_3$, respectively; in particular, the electronic structure of the $AlZr_3$ shows the strongest hybridization, leading to the worst ductility.

1. Introduction

Aluminum alloys represent an important category of materials because of their high technological value and their wide application, especially, in the aerospace field, microelectronics, motorized vehicles, and domestic industry. Due to the importance of the alloys in engineering and the basic research, mechanical behavior of the alloys has been a focus of various investigations. In particular, the strengthening for the alloys has attracted strong interest from both academic and industrial aspects. Over the past decades, various strengthening methods have been developed, e.g., alloying, and can solve the proposed issue. However, for other properties, such as corrosion or thermal resistance, such effectiveness is limit. Instead of the (micro amount) alloying method, a large amount of alloy elements can be used to form the so-called Al-based intermetallic compounds. It is found that such intermetallics can exhibit various excellent properties, including mechanical, physical, and chemical ones, because bonding nature or electronic structure are changed [1].

Intermetallics involving aluminum and transition metals (TM) are known to have high resistance to oxidation and corrosion, elevated-temperature strength, relatively low density, and high melting points, which making them desirable candidates for high-temperature structural applications [2]. In particular, zirconium can effectively enhance the mechanical strength of the alloys when copper and zinc elements exist in aluminum and Al-based alloys [3]. Adding Zr in the Al–Mg alloys can effectively

discard hydrogen, grain refinement, reducing pinholes, porosity and hot cracking tendency and improve its mechanical properties [4]. Many investigations have been focused on the constituent binary systems, such as Al–Cu, Al–Zr, and Cu–Zr [5–10], however, there has been a lack of systematic theoretical and experimental investigations for binary and ternary system, especially for ternary alloy system.

In recent years, first-principles calculations based on the density-functional theory have become an important tool for the accurate study of the crystalline and electronic structures and mechanical properties of solids [11]. In the present study, we report a systematic investigation of the structural, elastic and electronic properties of Al-based alloys ($AlCu_3$, $AlZr_3$, and $AlCu_2Zr$) by first-principles calculations, and the results are discussed in comparison with the available experimental data and other theoretical results.

2. Computational method

All calculations were performed using the Vienna *ab initio* Simulation Package (VASP) [12, 13] based on the density-functional theory (DFT) [14]. The exchange and correlation energy was treated within the generalized gradient approximation of Perdew–Wang 91 version (GGA-PW91) [15]. The interaction between the valence electrons and the ions was described by using potentials generated with Blöchl's projector augmented wave (PAW) method [16]. The PAW potential used for Al treats $3s$, $3p$ states as valence states, and the other electron–ion interaction was described by $3d$, $4s$ valence states for Cu, $5s$, $4d$, $5p$ valence states for Zr. A plane-wave energy cutoff was set at 450 eV for $AlCu_3$ and $AlCu_2Zr$, and at 350 eV for $AlZr_3$. The Brillouin zone integrations

*corresponding author

were performed using the Monkhorst–Pack [17] k-point meshes, e.g., the k-point meshes for AlCu$_3$, AlCu$_2$Zr and AlZr$_3$ were $15 \times 15 \times 15$, $9 \times 9 \times 9$ and $13 \times 13 \times 13$ for optimizing geometry and calculating elastic constants, and $25 \times 25 \times 25$, $19 \times 19 \times 19$ and $23 \times 23 \times 23$ for the calculations of density of states (DOS) at the equilibrium volume, respectively.

Optimizations of the structural parameters (atomic positions and the lattice constants) for each system were performed using the conjugate gradient method, and the coordinates of internal atoms were allowed to relax until the total forces on each ion were less than 0.01 eV/Å. The total energy and density of states (DOS) calculations were performed with the linear tetrahedron method with the Blöchl corrections [18]. In order to avoid wrap-around errors, all calculations were performed using the "accurate" setting within VASP.

3. Results and discussion

3.1. Equilibrium properties

AlCu$_3$ and AlZr$_3$ alloys have the simple cubic Cu$_3$Au ($L1_2$ type, space group Pm-$3m$) structure [19, 20], AlCu$_2$Zr crystallizes in cubic symmetry with the space group Fm-$3m$ [21]. Firstly, these crystal structures were optimized with relaxation of cell shape and atomic positions. The equilibrium volume V_0, bulk modulus B_0 and the pressure derivation of bulk modulus B_0' of AlCu$_3$, AlCu$_2$Zr, and AlZr$_3$ were determined by fitting the total energy calculated at different lattice constant values to a Birch–Murnaghan equation of state [22]. The results of first-principles calculations are listed in Table I. From Table I, one can see that the results of our calculations compare very favorably with experimental data. This shows that the used parameters are reasonable.

TABLE I

Calculated and experimental lattice parameters a (Å), equilibrium volume V_0 (Å^3), bulk modulus B_0 (GPa) and the pressure derivation of bulk modulus B_0' for AlCu$_3$, AlCu$_2$Zr, AlZr$_3$.

	AlCu$_3$		AlCu$_2$Zr		AlZr$_3$	
	present	exp.	present	exp.	present	exp.
a	3.693	3.607 [19]	6.256	6.216 [21]	4.381	4.392 [20]
V_0	50.358	–	244.805	240.210 [21]	84.110	84.700 [20]
B_0	131.010	–	128.600	–	100.800	
B_0'	4.47	–	4.280	–	3.48	

It is known that the stability of crystal structure is correlated to its cohesive energy [23], which is often defined as the work which is needed when crystal is decomposed into the single atom. Hence, the bigger the cohesive energy is, the more stable the crystal structure is [23]. In the present study, the cohesive energies (E_{coh}) of AlCu$_3$, AlCu$_2$Zr and AlZr$_3$ crystal cells can be calculated by

$$E_{\mathrm{coh}}^{\mathrm{ABC}} = (E_{\mathrm{tot}} - N_{\mathrm{A}}E_{\mathrm{atom}}^{\mathrm{A}} - N_{\mathrm{B}}E_{\mathrm{atom}}^{\mathrm{B}} - N_{\mathrm{C}}E_{\mathrm{atom}}^{\mathrm{C}})$$
$$\big/ (N_{\mathrm{A}} + N_{\mathrm{B}} + N_{\mathrm{C}}), \tag{1}$$

where E_{tot} is the total energy of the compound at the equilibrium lattice constant, and $E_{\mathrm{atom}}^{\mathrm{A}}$, $E_{\mathrm{atom}}^{\mathrm{B}}$, $E_{\mathrm{atom}}^{\mathrm{C}}$ are the energies of the isolated atoms A, B, and C in

the freedom states. N_{A}, N_{B}, and N_{C} refer to the numbers of A, B, and C atoms in each unit cell. The energies of isolated Al, Cu, and Zr atoms are -0.276 eV, -0.254 eV and -2.054 eV, respectively. Cohesive energies (E_{coh}) per atom of all crystal or primitive cells are calculated from Eq. (1). It was found for Al-based intermetallic compounds that the cohesive energy (E_{coh}) of per atom for AlCu$_3$, AlCu$_2$Zr and AlZr$_3$ are -3.637 eV, -4.551 eV, -5.964 eV, respectively. These results are listed in Table II. Based on the above results, it can be concluded that the cohesive energy of these Al-based intermetallic compounds will become lower with increasing Zr element in crystal, hence the stability of crystal increases. Therefore, the AlZr$_3$ intermetallic compound should have the highest structure stability, followed by AlCu$_2$Zr and finally the AlCu$_3$.

TABLE II

Total energy E_{tot}, cohesive energy E_{coh} and formation energy ΔH of AlCu$_3$, AlCu$_2$Zr, and AlZr$_3$.

Compound	E_{tot} [eV/atom]	E_{coh} [eV/atom]	ΔH [eV/atom]
AlCu$_3$	-3.897	-3.637	-0.177
AlCu$_2$Zr	-5.261	-4.551	-0.359
AlZr$_3$	-7.574	-5.964	-0.307

In order to compare the alloying abilities of the present compounds, we calculate the formation energy ΔH, which can be given by

$$\Delta H_{\mathrm{ABC}} = (E_{\mathrm{tot}} - N_{\mathrm{A}}E_{\mathrm{solid}}^{\mathrm{A}} - N_{\mathrm{B}}E_{\mathrm{solid}}^{\mathrm{B}} - N_{\mathrm{C}}E_{\mathrm{solid}}^{\mathrm{C}})$$
$$\big/ (N_{\mathrm{A}} + N_{\mathrm{B}} + N_{\mathrm{C}}), \tag{2}$$

where $E_{\mathrm{solid}}^{\mathrm{A}}$, $E_{\mathrm{solid}}^{\mathrm{B}}$, and $E_{\mathrm{solid}}^{\mathrm{C}}$ are the energies per atom of pure constituents A, B, and C in the solid states, respectively. The other variables are as defined for Eq. (1). Negative formation energies usually indicate an exothermic process. Furthermore, the bigger the formation energy is, the stronger alloying ability is [23]. The calculated energies of Al, Cu, and Zr in their respective crystals are -3.696 eV, -3.728 eV, -8.457 eV. The calculated results of these compounds are also listed in Table II. The formation energies of AlCu$_3$, AlCu$_2$Zr and AlZr$_3$ are all negative, which means that the structure of these phases can exist and be stable. The present results also indicate that AlCu$_2$Zr phase has the biggest formation energies, suggesting a strong alloying ability. It should be noted that the formation energies of AlZr$_3$ was larger than that of AlCu$_3$, indicating that the latter has a weaker alloying ability than the former. Here, cohesive energy and formation energies expected different trends in stability. Due to the higher cohesive energy of Zr, the cohesive energy of the alloys increases when the Zr content increases.

3.2. Mechanical properties

The density-functional theory has become a powerful tool for investigating the elastic properties of materials (in the limit of zero temperature and in the absence of zero-point motion). For a given crystal it is possible to calculate the complete set of elastic constants by apply-

ing small strains to the equilibrium unit cell and determining the corresponding variations in the total energy. The necessary number of strains is imposed by the crystal symmetry [24]. For a material with cubic symmetry, there are only three independent elastic constants, C_{11}, C_{12}, and C_{44}. The strain tensor is given by

$$\delta = \begin{pmatrix} \delta_{11} & \delta_{12} & \delta_{13} \\ \delta_{21} & \delta_{22} & \delta_{23} \\ \delta_{31} & \delta_{32} & \delta_{33} \end{pmatrix}. \tag{3}$$

In the present study, we applied three kinds of strains $\delta^{(N)}$ ($N = 1, 2, 3$) so as to obtain the elastic constants, and they are listed in Table III. The first strain is a volume-conserving tetragonal deformation along the z axis, the second refers to a uniform hydrostatic pressure, and the last one corresponds to a volume-conserving orthorhombic shear [24]. The elastic strain energy was given by

$$U = \frac{\Delta E}{V_0} = \frac{1}{2} \sum_{i=1}^{6} \sum_{j=1}^{6} C_{ij} e_i e_j, \tag{4}$$

where $\Delta E = E_{\text{total}}(V_0, \delta) - E_{\text{total}}(V_0, 0)$ is the total energy variation between the deformed cell and the initial cell, V_0 is the equilibrium volume of the cell, C_{ij} are the elastic constants and δ is the deformation added to the equilibrium cell. The elastic strain energy is also listed in Table III. For each kind of lattice deformation,

the total energy has been calculated for different strains $\gamma = \pm 0.01n$ ($n = 0–2$).

TABLE III

The strains used to calculate the elastic constants of AlCu$_3$, AlCu$_2$Zr, and AlZr$_3$, with $\gamma = \pm 0.01n$ ($n = 0–2$).

Strain	Parameters (unlisted $\delta_{ij} = 0$)	$\Delta E/V_0$ to O(γ^2)
$\delta^{(1)}$	$\delta_{11} = \delta_{22} = \gamma,\ \delta_{33} = [(1+\gamma)^{-2} - 1]$	$3(C_{11} - C_{12})\gamma^2$
$\delta^{(2)}$	$\delta_{11} = \delta_{22} = \delta_{33} = \gamma$	$\frac{3}{2}(C_{11} + 2C_{12})\gamma^2$
$\delta^{(3)}$	$\delta_{12} = \delta_{21} = \gamma,\ \delta_{33} = [\gamma^2(1-\gamma^2)^{-1}]$	$2C_{44}\gamma^2$

By means of polynomial fit, we extracted three values of the second order coefficients, corresponding to $3(C_{11}-C_{12})$, $3(C_{11}+2C_{12})/2$ and $2C_{44}$, respectively, the elastic constants C_{11}, C_{12}, and C_{44} were obtained [25], and the results are showed in Table IV. From Table IV, we can see that our calculation results agree well with the experimental data or other first-principle calculations. These elastic constants satisfy the requirement of mechanical stability for cubic crystals [24]: $(C_{11} - C_{12}) > 0$, $C_{11} > 0$, $C_{44} > 0$, $(C_{11} + 2C_{12}) > 0$. This shows that AlCu$_3$, AlCu$_2$Zr, and AlZr$_3$ have a stable structure. The average bulk modulus is identical to the single-crystal bulk modulus, i.e., $B = (C_{11} + 2C_{12})/3$. Interestingly, we noted that the bulk modulus calculated from the values of the elastic constants is in good agreement with the one obtained through the fit to a Birch–Murnaghan equation of state (B_0), giving a consistent estimation of the compressibility for these compounds [26].

TABLE IV

Calculated elastic constants (GPa) and elastic modulus (bulk modulus B (GPa), shear modulus G (GPa), Young's modulus E (GPa), Poisson's ratio ν and anisotropy constant A) of AlCu$_3$, AlCu$_2$Zr, and AlZr$_3$.

Compound	C_{11}	C_{12}	C_{44}	B	G	B/G	E	ν	A	Ref.
AlCu$_3$	150.707	120.565	81.880	130.612	43.593	2.996	117.686	0.350	1.887	this study
	176.000	117.400	92.400	136.900	49.600		132.800	0.340		[5]
AlCu$_2$Zr	157.504	115.305	62.685	129.371	41.237	3.137	111.829	0.356	1.528	this study
AlZr$_3$	148.653	79.387	70.834	102.476	53.400	1.919	136.492	0.278	1.487	this study
	163.800	79.300	86.500	107.670						[6]

In order to further validate our results, the elastic modulus, such as shear modulus G (GPa), Young's modulus E (GPa), Poisson's ratio ν and anisotropy constant A for a polycrystalline material were also calculated with the single-crystal elastic constants C_{ij}, all of these elastic modulus are shown in Table IV. In the present study, we adopted Hershey's averaging method [27], which has been known to give the most accurate relation between single-crystal and polycrystalline values for a cubic lattice [28]. According to this method, G is obtained by solving the following equation:

$$G^3 + \frac{5C_{11} + 4C_{12}}{8}G^2 - \frac{C_{44}(7C_{11} - 4C_{12})}{8}G$$
$$- \frac{C_{44}(C_{11} - C_{12})(C_{11} + 2C_{12})}{8} = 0. \tag{5}$$

The calculated shear modulus G for the AlZr$_3$ are the largest, while the quantities for AlCu$_2$Zr are less than for AlCu$_3$.

Pugh [29] found that the ratio of the bulk modulus to shear modulus (B/G) of polycrystalline phases can predict the brittle and ductile behavior of materials. A high and low value of B/G are associated with ductility and brittleness, respectively. The critical value which separates ductility from brittleness is about 1.75. From B/G calculated in Table IV we can see that all the B/G ratios are larger than 1.75. Therefore, AlCu$_3$, AlCu$_2$Zr and AlZr$_3$ have a good ductility. On the contrary, the biggest B/G ratio for AlCu$_2$Zr indicates that AlCu$_2$Zr is of very good ductility in these three Al-based alloys. AlCu$_3$ has an intermediate ductility, while AlZr$_3$ has a worst ductility.

Besides B/G, Young's modulus E and Poisson's ratio ν, are important for technological and engineering applications. Young's modulus is used to provide a measure of the stiffness of the solid, i.e., the larger the value of E, the stiffer the material [24]. According to Hershey's averaging method, Young's modulus is defined as: $E = 9GB/(3B + G)$. Based on the calculated results, we find that AlZr$_3$ has a Young modulus that is 18.806 GPa and 24.663 GPa larger than for AlCu$_3$ and AlCu$_2$Zr, respectively. This indicates that AlZr$_3$ phase has the highest stiffness, followed by AlCu$_3$ and finally the AlCu$_2$Zr. In addition, Poisson's ratio ν has also been used to measure the shear stability of the lattice, which usually ranges from -1 to 0.5. The greater the value of Poisson's ratio ν, the better the plasticity of the materials. So we can see that AlCu$_3$, AlCu$_2$Zr and AlZr$_3$ have a better plasticity.

The elastic anisotropy of crystals has an important application in engineering materials since it is highly correlated with the possibility of inducing microcracks [24, 30]. For cubic symmetric structures [31], the elastic anisotropy is defined as $A = (2C_{44} + C_{12})/C_{11}$. For the completely isotropic material, the value of A will be 1, while values smaller or bigger than 1 measuring the degree of elastic anisotropy [24]. Interestingly, we note that the values of A (Table IV) do not deviate far from unity, suggesting that the present cubic structure alloys also do not deviate far from being isotropic. The calculated results also indicate that AlCu$_3$ is much more anisotropic than the other two alloys.

3.3. Density of the states

For further understanding of the electronic characteristics and structural stability, total density of states (DOS) of AlCu$_3$, AlCu$_2$Zr and AlZr$_3$ were calculated, as shown in Fig. 1, as well as the partial density of states (PDOS) of Al, Cu and Zr atoms in these Al-based intermetallics compounds. In Figure 1 there is evident the metallic character of these considered AlCu$_3$, AlCu$_2$Zr, and AlZr$_3$ structure because of the finite DOS at the Fermi level. With regard to the total density of states curve of AlCu$_3$, one can see from Fig. 1a that the whole valence band of AlCu$_3$ is located between -7 eV and 9 eV, which is dominated by Cu $3d$ states and a small contribution from $3s$ and $3p$ states of Al. The valence band of AlZr$_3$ (see Fig. 1c) can be divided into three areas. The first area dominated by the valence electron numbers of Al $3s$ and Zr $4d$ states are mostly located between -7 eV and -5 eV, the second by the Zr $5s$ and $4d$ states located between -4 eV and -3 eV, and the third by Zr $4d$ states located between -2.8 eV and 3.0 eV. Both below and above the Fermi level, the hybridization between Al p states and Zr d states is strong. Due to the strong hybridization (or covalent interaction) the entire DOS can be divided into bonding and antibonding regions, and that a pseudogap resides in between. The characteristic pseudogap around the Fermi level indicates the presence of the directional covalent bonding.
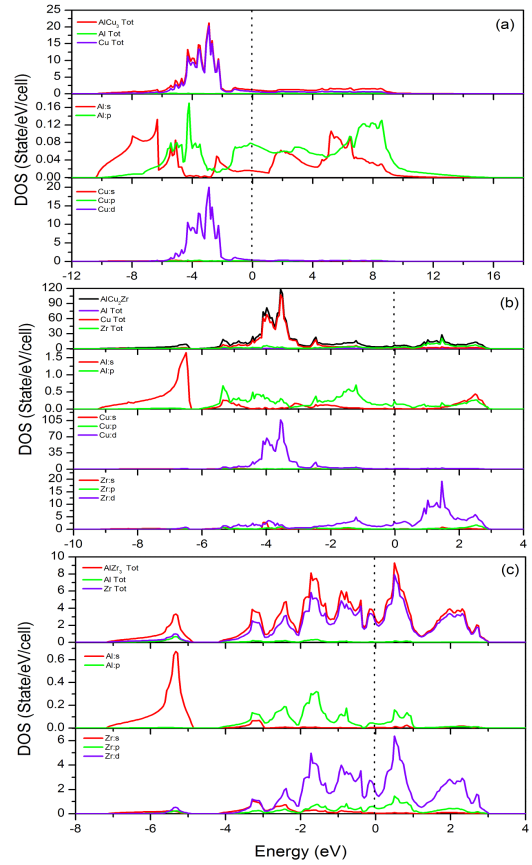
Fig. 1. The total and partial DOS of AlCu$_3$ crystal cell (a), AlCu$_2$Zr crystal cell (b), AlZr$_3$ crystal cell (c). The vertical dot line indicates the Fermi level.

The Fermi level located at a valley in the bonding region implies the system has a pronounced stability. It is also generally considered that the formation of covalent bonding would enhance the strength of material in comparison with the pure metallic bonding [32]. According to the covalent approach, the guiding principle is the maximize bonding. Therefore, for a series of compounds having the same structure, the greater the occupancy in the bonding region the higher the stability [33]. It is indeed seen that the structural stability increases from AlCu$_3$ to AlZr$_3$. For AlCu$_2$Zr (see Fig. 1b), it is found that the main bonding peaks between -6 eV and -2 eV are predominantly derived from the Cu $3d$ orbits, while the main bonding peaks between the Fermi level and 3 eV predominantly derived from the Zr $4d$ orbits. It should be noted that the phase stability of intermetallics depends on the location of the Fermi level and the value of the DOS at the Fermi level, i.e. $N(E_F)$ [34, 35]. A lower $N(E_F)$ corresponds to a more stable structure. The value of the total DOS at the Fermi level is 3.64 states/eV for AlZr$_3$. The value of the total DOS at the Fermi level is 5.74 states/eV for AlCu$_2$Zr. Therefore, AlZr$_3$ has a more stable structure in these three Al-based intermetallics. This accorded with the calculation of cohesive energy.

From Fig. 1, one can also see that the pseudogap or quasigap near the Fermi energy is the broadest for $AlZr_3$, and the narrowest for $AlCu_2Zr$, which suggests that $AlZr_3$ has the strongest covalent bond, $AlCu_3$ has an intermediate covalent bond, while $AlCu_2Zr$ has the worst covalent bond, i.e., $AlZr_3$ may have the worst ductility among these three Al-based intermetallics, $AlCu_3$ has an intermediate ductility, while $AlCu_2Zr$ has most ductility.

According to the partial DOS, the large occupied peak for the $AlCu_3$, $AlCu_2Zr$, $AlZr_3$ alloys is dominated by Al $3s$ and $3p$ states, Cu $3d$ states, Zr $5s$ and $4d$ states, respectively. In the valence band range, there is hybridization in these alloys, and $AlZr_3$ has the strongest hybridization in these three Al-based intermetallics. This is an advantage for ductility of $AlZr_3$ alloy. However, from the above analysis, it can be seen that the pseudogap or quasigap near the Fermi energy for $AlZr_3$ is the broadest among these Al-based alloys. This is a disadvantage for ductility of $AlZr_3$. Thus, the ductility of $AlZr_3$ alloy may be less than that of $AlCu_3$ and $AlCu_2Zr$ alloys.

4. Conclusions

In summary, using the first-principles method we have calculated alloying stability, electronic structure, and mechanical properties of Al-based intermetallic compounds ($AlCu_3$, $AlCu_2Zr$, and $AlZr_3$). The calculation of cohesive energies showed that the structural stability of these Al-based intermetallics will become higher with increasing Zr element in crystal. The calculation of formation energies showed that the alloying ability of $AlCu_2Zr$ is strongest. $AlCu_2Zr$ can exhibit a good ductility, followed by $AlCu_3$, whereas $AlZr_3$ can have a poor ductility; however, for stiffness, these intermetallics show a converse order. In particular, $AlCu_3$ is much more anisotropic than the other two intermetallics. The valence bonds of these intermetallics are attributed to the valence electrons of Cu $3d$ states for $AlCu_3$, Cu $3d$, and Zr $4d$ states for $AlCu_2Zr$, and Al $3s$, Zr $5s$ and $4d$ states for $AlZr_3$, respectively, and the electronic structure of the $AlZr_3$ shows the strongest hybridization, leading to the worst ductility.

References

[1] G. Sauthoff, in: *Intermetallic Compounds*, Eds. J.H. Westbrook, R.L. Fleischer, Vol. 1, Wiley, New York 1994, p. 991.

[2] R.W. Cahn, *Intermetallics* **6**, 563 (1998).

[3] P.K. Rajagopalan, I.G. Sharma, T.S. Krishnan, *J. Alloys Comp.* **285**, 212 (1999).

[4] P. Wonwook, *Mater. Design* **17**, 85 (1996).

[5] W. Zhou, L.J. Liu, B.L. Li, Q.G. Song, P.J. Wu, *Electron Mater.* **38**, 356 (2009).

[6] C. Emmanuel, J.M. Sanchez, *Phys. Rev. B* **65**, 094105 (2002).

[7] G. Ghosh, M. Asta, *Acta Mater.* **53**, 3225 (2005).

[8] G. Ghosh, *Acta Mater.* **55**, 3347 (2007).

[9] W.J. Ma, Y.R. Wang, B.C. Wei, Y.F. Sun, *Trans. Nonferrous Met. Soc. China* **17**, 929 (2007).

[10] S. Pauly, J. Das, N. Mattern, D.H. Kim, J. Eckert, *Intermetallics* **17**, 453 (2009).

[11] H. Baltache, R. Khenata, M. Sahnoun, M. Driz, B. Abbar, B. Bouhafs, *Physica B* **344**, 334 (2004).

[12] G. Kresse, J. Hafner, *Phys. Rev. B* **49**, 14251 (1994).

[13] G. Kresse, J. Furthmüller, *Phys. Rev. B* **54**, 11169 (1996).

[14] W. Kohn, L.J. Sham, *Phys. Rev.* **140**, A1133 (1965).

[15] J.P. Perdew, Y. Wang, *Phys. Rev. B* **45**, 13244 (1992).

[16] P.E. Blöchl, *Phys. Rev. B* **50**, 17953 (1994).

[17] H.J. Monkhorst, J.D. Pack, *Phys. Rev. B* **13**, 5188 (1976).

[18] P.E. Blöchl, O. Jepsen, O.K. Andersen, *Phys. Rev. B* **49**, 16223 (1994).

[19] M. Draissia, M.Y. Debili, N. Boukhris, M. Zadam, S. Lallouche, *Copper* **10**, 65 (2007).

[20] W.J. Meng, J. Faber, Jr., P.R. Okamoto, L.E. Rehn, B.J. Kestel, R.L. Hitterman, *J. Appl. Phys.* **67**, 1312 (1990).

[21] R. Meyer zu Reckendorf, P.C. Schmidt, A. Weiss, *Z. Phys. Chem. N.F.* **163**, 103 (1989).

[22] F.J. Birch, *Geophys. Res.* **83**, 1257 (1978).

[23] V.I. Zubov, N.P. Tretiakov, J.N. Teixeira Rabelo, *Phys. Lett. A* **194**, 223 (1994).

[24] M. Mattesini, R. Ahuja, B. Johansson, *Phys. Rev. B* **68**, 184108 (2003).

[25] W.Y. Yu, N. Wang, X.B. Xiao, B.Y. Tang, L.M. Peng, W.J. Ding, *Solid State Sci.* **11**, 1400 (2009).

[26] B.Y. Tang, N. Wang, W.Y. Yu, X.Q. Zeng, W.J. Ding, *Acta Mater.* **56**, 3353 (2008).

[27] H.M. Ledbetter, *J. Appl. Phys.* **44**, 1451 (1973).

[28] A. Taga, L. Vitos, B. Johansson, G. Grimvall, *Phys. Rev. B* **71**, 014201 (2005).

[29] S.F. Pugh, *Philos. Mag.* **45**, 823 (1954).

[30] V. Tvergaard, J.W. Hutchinson, *J. Am. Ceram. Soc.* **71**, 157 (1988).

[31] B.B. Karki, S. Stixrude, S.J. Clark, M.C. Warren, G.J. Ackland, J. Crain, *Am. Miner.* **82**, 51 (1997).

[32] P. Chen, D.L. Li, J.X. Yi, W. Li, B.Y. Tang, L.M. Peng, et al., *Solid State Sci.* **11**, 2156 (2009).

[33] J.H. Xu, W. Lin, A.J. Freeman, *Phys. Rev. B* **48**, 4276 (1993).

[34] J.H. Xu, T. Oguchi, A.J. Freeman, *Phys. Rev. B* **36**, 4186 (1987).

[35] T. Hong, T.J. Watson-Yang, A.J. Freeman, T. Oguchi, J.H. Xu, *Phys. Rev. B* **41**, 12462 (1990).